Single Side-Band Modulation Performance of a LiNbO₃ Integrated Modulator Consisting of Four-Phase Modulator Waveguides

S. Shimotsu, S. Oikawa, T. Saitou, N. Mitsugi, K. Kubodera, T. Kawanishi, and M. Izutsu

Abstract-Single side-band (SSB) technologies are especially useful in optical fiber communication systems, such as higher density wavelength multiplexing and long-haul fiber transmission due to less nonlinear optical effects, because of the reduced optical power. This letter reports on the SSB modulation performance of a LiNbO₃ integrated modu]ator consisting of four phase modulator waveguides. Optical SSB modulation with suppressions of main carrier (–22.6 dB) and J_3 subcarrier (-18.4 dB) of a 10-GHz single-tone signal with a driving voltage of 6.3 V_{p-p} was demonstrated. The total insertion loss was l0.6 dB.

Index Terms-Microwave modulation , modulation , optical modulation, optical single side-band modulation, optical waveguides, single side-band, waveguides.

I. INTRODUCTION

T HE expansion of Internet and wireless communications has prompted research into dense wavelength division multiplexing (D-WDM). Several functional devices have intended for rea]ization of D-WDM networks have been developed for wa\'e.length ranges from 1 528 to 1561 nm (C-band), and from 1570 to 1610 nlTl (L-band) [l].

Among these devices, LiNbO₃ (LN) modulators are indispensable for high-bit-rate D-WDM systems because they can operate over a wide wavelength range and frequency range. Since LN modulators designs vary using waveguided phase modulators, Mach-Zehnder (MZ) interferometers, *Y* branches, and cross-junction couplers, they are also promising as key devices for several kinds of optical modulation systems. These include CATV modulators with complimentaly outputs [2] and return-to-zero (RZ) pulse modulators consisting of two MZ modulators [3].

In addition to the above-mentioned fiber communication system devices, LN modulators have application to radio communication system devices, such as optical sub-carrier generators, frequency shifters, and single side-band (SSB) modulators [4]-[6]. SSB technologies are especially useful in digital optical fiber communication systems [7], [8], such as higher density wavelength multiplexing and longer haul fiber transmission. SSB technologies can suppress nonlinear optical
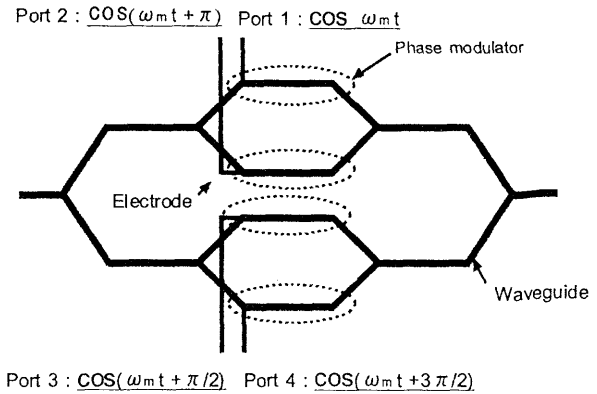
Fig l. Schematic diagram of an integrated LiNbO₃ four balanced phase modulators. Bolded lines show waveguides. and fine lines show electrodes.

effects because of the reduced optical power to demonstrate the potential of LN modulators [9], [10]. Our proposed configuration can generate a single side-band suppression carrier (SSB-SC) signal. The modulation signal can be detected by mixing a carrier signal of *a local oscillator*. We fabricated an LN integrated modulator consisting of four phase modulation waveguides and tested its performance in an SSB modulation experiment.

II. PRINCIPLES OF OPERATION

The integrate.d modulator consists of parallel Mach-Zehnder intensity modulators , i.e., four optical phase modulator waveguides as shown in Fig. 1. Electrical signals applied to each of the four phase modulators are respectively cosωmt, cos (ωmt + π) , cos(ωmt + π /2) , cos(ωmt + 3π/2.) . The optical output signal for in-phase modes is

$$f_1(t) = AJ_{-1}(m_f)\cos(\omega_c - \omega_m)t - AJ_3(m_f)$$
$$\times \cos(\omega_c + 3\omega_m)t \quad (1)$$

and that for out-of-phase modes is

$$f_2(t) = AJ_1(m_f)\cos(\omega_c + \omega_m)t - AJ_{-3}(m_f)$$
$$\times \cos(\omega_c - 3\omega_m)t \quad (2)$$

Where

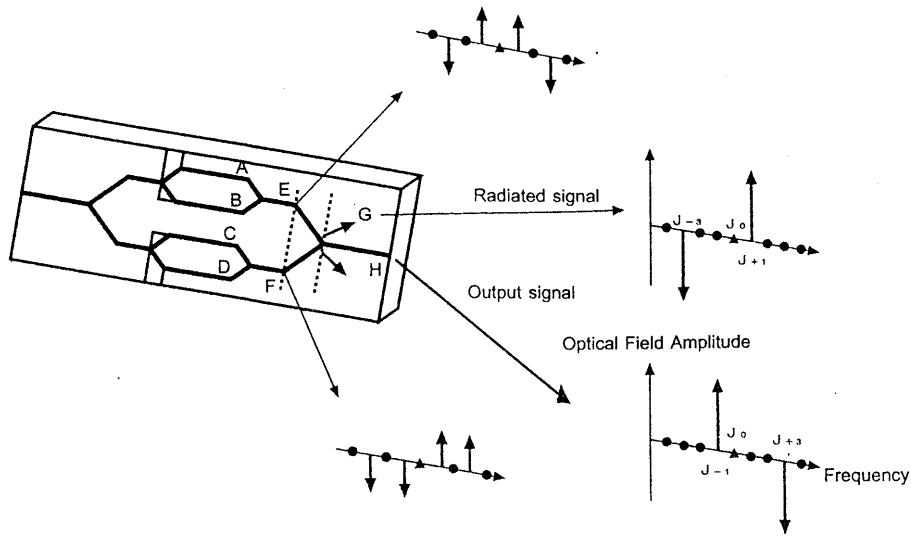|	
ω_c	optical carrier angular frequency:
ω_m	modulation angular frequency:
ω_f	modulation index.

Fig. 2. Principle of the SSB modulation. Each frequency diagram sho\vs Bessel function profies of J_{-4} to J_4. Solid triangles show main carrier J_0 and solid circles show modes that cancel each other out.
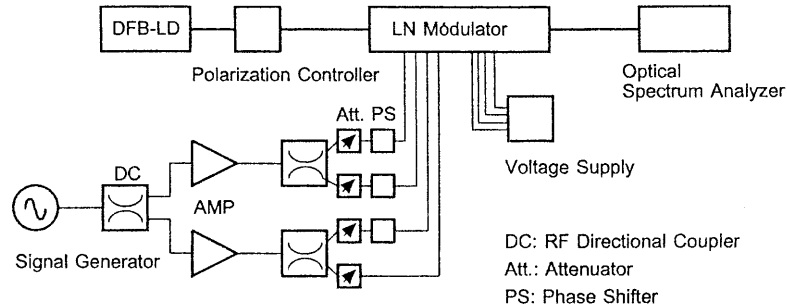

Fig.3 Block diagrams of the. SSB modulation measurerment. A 10-GHz single-tone signal was used for the modulation s ignal.

Equations (1) and (2) reveal that the optical carrier frequency is shifted by the modu]ation frequency ω_m and that two sets of optical subcarriers with frequency spacing $4\omega_m$ are produced. Only in-phase modes (J_{-1} and J_3) propagate through the Y-junction as the output signal, and out-of-phase modes (J_1 and J_{-3}) radiate from the waveguide at the Y junction.

Fig. 2 illustrates the Bessel function profiles for the output signal (H), the radiated signal (G), and signals at Y junctions (E and F), where the four wave guides (A, B, C, D) are modulated by signals $\cos\omega_m t$, $\cos(\omega_m t + \pi)$, $\cos(\omega_m t + \pi/2)$, $\cos(\omega_m t + 3\pi/2)$, respectively.

III. EXPERIMENTS AND DISCUSSIONS

A. Device Fabrication [11], [12]

An LN modulator with the structure. shown in Fig. I was fabricated on a LiNbO3 Substrate. Waveguides were formed on a z-cut substrate by titanium diffusion. The substrate was coated with a buffer layer of silicon dioxide. A gold coplanar-waveguide (CPW) traveling-wave type electrode was formed on the buffer layer. The lengths of electrodes for ports 1-4 were 40 mm. The modulator was pigtailed with polarization maintaining (PANDA) fibers using an ultraviolet cured adhesive and was electrically connected by GPO connectors. A polarizer was placed at the optical output port.

The modulation bandwidths for ports 1-4 were measured to be more than 20 GHz. The half wavelength voltage $V\pi$ for ports 1-4 were 4.7 V at DC and 5.4 V at 10 GHz. The optical insertion loss, including waveguide propagation loss, Y-branch loss, and connection loss between the waveguide and fibers was 5.9 dB.

B. SSB Modulation Performance

Fig. 3 shows the experimental setup of the optical SSB modulation. A 10-GHz single-tone signal was used for the modulation. It was divided into four signals by three RF directional couplers. The RF attenuators and RF phase shifters adjusted the amplitudes and phases of signals. DC bias voltages were applied to ports 1-4 to adjust the optical phases. It has a difference of an optical path length in MZ structure. Optical output spectra were measured with an optical spectrum analyzer.

Fig. 4 shows the optical spectrum of the sideband generation with sideband suppression, where an RF drive voltage V_{p-p} was applied to ports 1-4 to make the J_{-1} mode power maximum. A spectrum of DFB-LD output is also shown in the figure. Sidebands J_{-1} and J_3 are shown in the figure. The suppression ratio between J_{-1} and J_3 Was 18.4 dB.
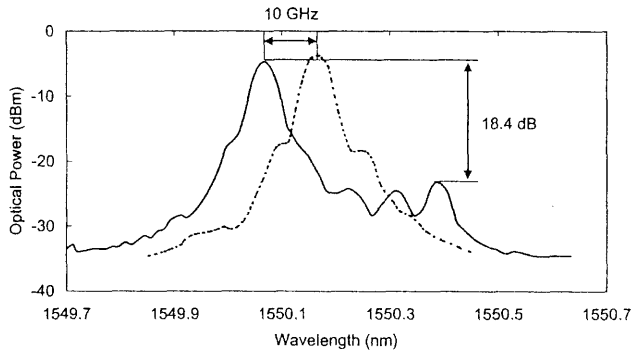
Fig. 4 Measured optical spectrum of the SSB modulation. The dotted line shows a spectrum of a DFB-LD.
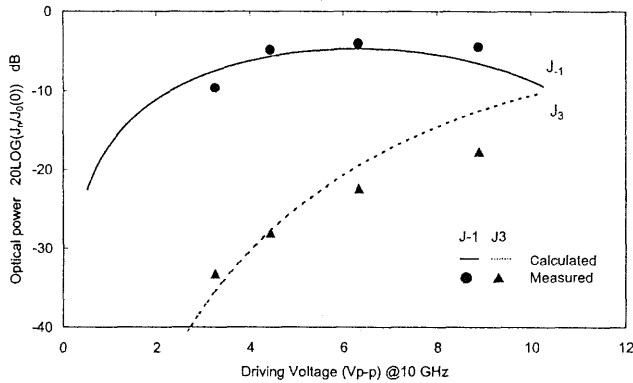

Fig. 5. Relationship between optical power for J_{-1} and J_3 modes and driving voltage. Solid line and circles show the calculated and measured of J_{-1} values, dotted line and triangles show the calculated and measured of J_3 values . J_0 (0) means the optical power of the main carrier J_0 without the RF voltage.

Optical field amplitudes of the negative first- and third-order elements J_{-1} and J_3 are shown in Fig. 5 together with theoretical values calculated by (1). As shown in the figure, they show a good agreement. The negative first-order element (J_{-1}) shows maximum optical power at the driving voltage of 6.3 V. This means the best power efficiency at this point.

IV. CONCLUSION AND DISCUSSION

Optical SSB modulation with the suppression of the main carrier and J_3 subcarrier (-18.4 dB) of a 10 GHz. single-tone signal with a driving voltage of 6.3 V_{p-p} was carried out using a LiNbO$_3$ integrated modulator consisting of four phase modulators. The total optical insertion loss was 10.6 dB, including the estimated 5.9-dB waveguide propagation loss and the 4.7-dB

Bessel-function conversion loss from J_0 to J_1.

SSB modulation will be useful in several optical communication applications such as high-bit-rate long-haul fiber transmission systems, high-density subcarrier multiplexes for fiber- radio communication systems, and optical frequency shifters and/or frequency switches of future WDM photonic network systems.

REFERENCES

[1] T. Ito et al., "3.2 Tb/s 1500 km WDM transmission experiment using 64 nm hybrid repeater amplifiers," presented at the OFC 2000, Paper PD-24.
[2] D. Piehler et al., "55 CIB CNR over 50 km of fiber in an 80-channel externally-modulated AM-CATV system without optical amplification," Electron. Lett , vol. 33, no. 3, pp. 226-227, 1997.
[3] Ed. L. Wooten et al., "A review of lithium niobate modulators for fiber-optic communications systems," IEEE J. Select. Topics Quantum Electron., vol. 6. pp. 69-82, 2000.
[4] M. Izutsu. S. Shikama, and T. Sueta, "Integrated optical SSB Modulator/frequency shifter," IEEE J. Quantum Electlon., vol. QE-17, pp. 2225-2227, Nov. 1981.
[5] S. Shimotsu et al., "Sub-carrier generation with integrated four balanced LiNbO$_3$ phase modulators," presented at the IEICE-2000, Paper C-3-20, Hiroshima, Japan.
[6] S. Shimotsu el al., "LiNbO$_3$ optical single-sideband modulator," presented at the OFC 2000, Paper PD- 16.
[7] H. Ogawa, D. Polifko, and S. Banba, "Millimeter-wave fiber optics systems for personal radio communication," IEEE Trans. Microwave Theory Tec., vol. 40, pp. 2285-2293, 1992.
[8] K. Horikawa, Y. Nakasuga, and H. Ogawa, "Self-heterodyning opiical waveguide beam forming and steering network integrated on lithium niobate substrate," IEEE Trans. Microwave Theory Tech , vol. 41, pp. 2395-2401. 1995.
[9] D. Novak et al., "Microwave and millimeter-wave photonic technologies for future fiber-radio communication systems." in Proc. CPT, 2000, pp. 53-56.
[10] Y. Miyamoto et al., "320 Gbit/s (8 x 40 Gbit/s) WDM transmission over 367-km zero-dispersion-flattened line with 120-km repeater spacing using carrier-suppressed return-to-zero pulse format," Tech. Dig. Opt. Amplifire and Their Applicat., June 1999.
[11] K. Noguchi, O. Mitomi, and H. Miyakawa, "Millimeter-wave Ti: LiNbO$_3$ optical modulators," J. Lightwave Technol., vol. 16, pp. 615-619, 1998.
[12] S. Shimotsu et al., "Characteristics of LiNbO$_3$ high speed modulators." IEICE Trans. Commun., pp. 25-30. 1995.